Int. J. Heat Mass Transfer. Vol. 16, pp. 567–580. Pergamon Press 1973. Printed in Great Britain

HEAT TRANSFER THROUGH THE UNSTEADY LAMINAR BOUNDARY LAYER ON A SEMI-INFINITE FLAT PLATE

PART II: EXPERIMENTAL RESULTS FROM AN OSCILLATING PLATE

NORMAN A. EVANS*

Gas Dynamics Laboratory, Forrestal Campus, Princeton, N.J., U.S.A.

(*Received* 23 *February* 1972 *and in revised from* 17 *July* 1972)

Abstract—An externally heated ceramic flat plate, instrumented on both surfaces with short time response platinum film resistance thermometers, was used to compare the amplitude of the additional unsteady heat transfer rate, δq_w, during oscillation in its own plane in a steady parallel air stream, of velocity U_∞, with the corresponding steady state heat transfer rate, q_{ws}, without oscillation.

The plate oscillation frequency, f, was varied between 1 and 60 Hz, the corresponding range of the Strouhal number, $S = \omega x/U_\infty$ ($\omega = 2\pi f$, x is the distance from the leading edge) being 0·006–20, and that of the velocity ratio, $\epsilon = u_{pmax}/U_\infty$ (u_{pmax} is the maximum plate velocity) being 0·005–6·5.

Amplification of periodic electrical signals corresponding to temperature amplitudes in the range 0·003–0·04°F showed that the qualitative trends of several existing theories for the behavior and phase shift (with respect to $u_{p_{max}}$) of H/ϵ (where $H = \delta q_w/q_{ws}$) for both small and large S, were substantiated by the experiment. H/ϵ was essentially constant and in phase for $S < 1{\cdot}5$, whereas, for $S > 1{\cdot}5$, $H/\epsilon \propto 1/S$ with the phase lag progressively approaching 90°. In addition, for a limited number of tests, no change in steady state heat transfer rate was detectable up to a value of $S = 2$.

NOMENCLATURE

A-N,	airstream surface film number at station N;
B-N,	shielded surface film number at station N;
f,	frequency [Hz];
H,	maximum heat transfer ratio;
k,	thermal conductivity;
Nu,	Nusselt number;
Pr,	Prandtl number;
q,	heat-transfer rate;
r,	crank radius of oscillatory drive;
R,	electrical resistance;
Re,	Reynolds number;
S,	Strouhal number;
t,	time;
t_p,	$2\pi/\omega$;
T,	temperature;
ΔT,	$T_w - T_\infty$, steady state temperature difference across plate thickness;
$\delta T(t)$,	unsteady surface temperature superimposed on T_w;
$\delta_1 T$,	amplitude of unsteady surface temperature;
U,	velocity;
u_p,	plate velocity during oscillation;
x,	distance from leading edge of plate;
y,	distance normal to plate surface;
λ,	correlation factor;
ϵ,	$u_{p_{max}}/U_\infty$;
μ,	coefficient of viscosity;
ρ,	density;
χ,	ceramic thermal diffusivity;
ϕ,	phase angle;

* Present address: Towne School of Civil and Mechanical Engineering, University of Pennsylvania, Philadelphia, Pa.
This work was carried out under sponsorship from the Fluid Mechanics Division of the Air Force Office of Scientific Research.

ω,	circular frequency [rad s^{-1}];
$\partial T/\partial n$,	normal surface temperature gradient.

Subscripts

A,	pertaining to airstream surface;
B,	pertaining to shielded surface;
s,	steady;
u,	unsteady maximum value;
w,	wall;
∞	condition in the free stream;
T,	pertaining to temperature;
Q,	pertaining to heat transfer rate.

1. INTRODUCTION

THE LAST fifteen years have seen an ever-increasing amount of attention to problems of unsteady fluid mechanics. Important examples that have been successfully tackled include rocket combustion instability and unsteady atmospheric re-entry, while continuing challenges include the possibility of improving the efficiency of heat exchangers.

Regarding the experimental side of unsteady boundary-layer flows, it appears that the only class of problems reasonably amenable to laboratory investigation is that associated with oscillating phenomena, and the pertinent literature appears to be almost exclusively concerned with this particular type of unsteadiness. Nickerson [1] and Hill and Stenning [2] used hot wire anemometry to check successfully the validity of theoretical predictions for the shape of the unsteady velocity profile in flat plate type configurations, and a recent presentation [3] on transition in oscillating boundary layers contains a large number of references, both theoretical and experimental.

It appears that work on unsteady heat transfer has dealt entirely with time-averaged observations, the objective being to determine the effect of oscillatory unsteadiness on the time-averaged heat transfer. In the mid-fifties, certain reviews [4, 5] indicated conflicting findings from several investigators, but since that time, a clearer picture of the subject has emerged. Romie [6] using turbulent pulsating pipe flow, found heat transfer changes dependent on the frequency, while Nickerson [1] experimentally checked (up to 10 Hz) his own analysis that oscillation of a flat plate changes the heat transfer to only a non-measurable extent. Up to 300 per cent increase in heat transfer has been measured in oscillating pipe flow by Harrje *et al.* [7–10], and attributed to complicated three-dimensional effects. Heated wires vibrated in transverse [11] and parallel [12] air flows produced significant heat transfer increases, while the addition of acoustic energy, has also increased the heat transfer rate [13, 14].

The effect of large amplitude velocity oscillations on the heat transfer from a heated plate was reported by Feiler and Yeager [15] who found up to 65 per cent increase in Nusselt number, with no effect attributable solely to frequency. An extensive bibliography and a tested proposal for heat exchanger improvement was given by Lemlich [16].

It is now well established experimentally that oscillation, under favorable circumstances, can significantly change the net heat-transfer level, but the published results are largely of an empirical nature, and existing theories are not capable of predicting the observed increases. The experiment to be described was conducted to test the validity of the theoretical predictions given in Part I [17], as follows. Let $q_{ws}(x)$ denote the heat transfer rate at point x from the plate leading edge where the free stream velocity U_∞ is steady and the surface is maintained at constant temperature. Correspondingly, let $\delta q_w(x, t)$ be the *additional* heat transfer rate due to an unsteady motion given by $U(t) = U_\infty\ (1 + \epsilon\, e^{i\omega t})$ where t is time, ω is a circular frequency and $\epsilon \ll 1$ is a non-dimensional constant. Putting $\delta q_w/q_{ws} = h$, then for Prandtl number $Pr = 0{\cdot}72$ and small Strouhal number $S = \omega x/U_\infty$, the result from Part I [17] is $h = (0{\cdot}5 - BiS)\, e^{i\omega t}$ where B is a small constant. The values of B from the analysis of various investigators are:

B	Investigator	Method
0·03	Lighthill	momentum integral
0·07	Illingworth	expansion in S
0·069	Ostrach	series in $\zeta_n = \dfrac{x^{n+1} U(t)^{(n+1)}}{U(t)^{n+2}}$
0·069	Evans	expansion in $\xi_0 = \left(\dfrac{x}{\int_0^t U(t)\,\mathrm{d}t}\right)^{\frac{1}{2}}$

For large S, Illingworth found $h/\epsilon = (0{\cdot}3945/iS) \times e^{i\omega t}$ using an expansion in $S^{-\frac{1}{2}}$.

In particular, if $\delta_1 q_w$ is the maximum value (amplitude of $q_w(x, t)$ and $H = \delta_1 q_w/q_{ws}$: $H/\epsilon = 0{\cdot}5$ very closely for small s, and is approximately in phase with $U(t)$, and $H/\epsilon = 0{\cdot}3945/S$ for large S and lags $U(t)$ by a phase angle $\phi_Q = 90°$. In addition, for a cycle period t_p,

$$\frac{1}{t_p}\int_0^{t_p} \delta q_w(x, t)\,\mathrm{d}t = 0$$

for both small and large S.

Thus, with no prediction of any change in the time-averaged heat-transfer level, it was necessary to investigate the time-wise details of the heat-transfer process, requiring temperature indicating instrumentation with a short response time. The model used was an externally heated ceramic flat plate, equipped with a sufficient number of platinum film thermometers to determine the steady heat transfer and the corresponding additional unsteady heat transfer under plate oscillation, using air as the fluid medium. The experiment was conducted entirely on the basis of observations of the surface temperature of a solid body when transferring heat to a fluid flowing over it.

2. OUTLINE OF THE EXPERIMENTAL PROGRAM AND PRACTICAL LIMITATIONS

The theoretical results given above as

$$H = H(\epsilon, S, \phi_Q)$$

require that both the stream temperature T_∞ and the plate surface temperature T_w be constant. However, the experimental arrangement to be described below would not allow constant $\Delta T = T_w - T_\infty$, but produced $\Delta T \propto x^{\frac{1}{2}}$ approximately. It is readily shown with constant U_∞ that $\Delta T \propto x^{\frac{1}{2}}$ gives rise to constant q_{ws}. Similarly, using equations (4.1) and (4.2) of [18] for no dissipation on a flat plate with $\Delta T \propto x^{\frac{1}{2}}$, it may be shown that the unsteady part of the heat transfer rate is also independent of x explicitly, but it does involve ϵ and S, so that a relation of the form $H = H(\epsilon, S, \phi_Q)$ will still hold.

A second experimental deviation from the theoretical requirements lay in the type of oscillatory plate motion employed. This was not truly sinusoidal, being derived from a slider-crank arrangement, and is described in more detail in Section 3.

The non-constant surface temperature, $T_w(x)$, resulted from the convenient use of carefully adjusted infra-red lamps to heat the model on one surface with an almost constant radiant energy flux. For a given value of U_∞, the value of ΔT near the plate trailing edge was set to a desired level by adjusting the power of the heating lamps, and accepting the equilibrium surface temperature produced with the plate at rest. $\Delta T(x)$ of the unheated surface was then measured, together with the temperature difference, $\Delta_1 T(x)$, across the plate thickness. The surface temperature gradient $(\partial T/\partial n)_s(x)$ was then obtained, using the Schwarz–Christoffel transformation to take into account the effects of conduction within the model.

With the same experimental conditions prevailing, the plate was oscillated at a desired frequency, and from the recorded local time variation in surface temperature, the value of $(\partial T/\partial n)_u(x)$ was computed, using Fourier analysis and the value of the thermal diffusivity of the plate material measured in the laboratory. Hence, there followed $H = (\partial T/\partial n)_u/(\partial T/\partial n)_s$ without the necessity of knowing the thermal conductivity of the plate material.

This method of reducing the unsteady data by Fourier analysis precluded determination of the leading (constant) term which represented, if non-zero, the change in net heat transfer due to oscillation. However, an independent sensitive method was used to detect its possible existence, although there is no prediction of it from theoretical considerations.

As shown in [19], a plate thickness above a certain minimum allows "separation" of the temperature effects on the opposite faces, thus considerably facilitating the determination of $(\partial T/\partial n)_u$ at the surface of interest. The separation effect is further accentuated by low values of the material thermal diffusivity, which, at the same time, improves the temperature sensitivity of the platinum film thermometry and increases the magnitude of the steady state temperature difference across the thickness.

3. APPARATUS

The basic model was fired, ground and polished in the laboratory from a self-glazing opaque ceramic slip (trade name: Parian) with final dimensions 3 in. long, 2·5 in. wide by 0·100 in. thick, and a 15° flat bevelled leading edge terminating in a thickness of 0·0015 in. The heat transfer of interest occurred from the non-bevelled airstream surface (designated surface *A*), while the other surface (designated surface *B*) was heated externally by infra-red lamps, as described below. The onset of boundary layer transition on surface *A* was delayed by the addition of a blunted, tangent-ogive shaped plexiglass nose-piece which extended the leading edge forward by 0·25 in. (Fig. 1). In addition, the sting-mounted model was fitted with a 1 in. long, smooth-sanded balsa trailing edge extension to remove, as far as practically possible, the influence of the trailing edge wake, during oscillation, from the rear portion of the ceramic section of the model.

The model was instrumented with thin (0·1 μ), fast response (1 MHz) platinum film thermometers (fired from Hanovia 05 liquid bright platinum paint), each approximately 0·5 in. long by 0·005 in. wide with a resistance of 950 Ω, and positioned on both surfaces every 0·25 in. symmetrically across the long center line, starting from the ceramic sharp edge. These were mirror-like in appearance, and were designated *A*-0 to *A*-11 on surface *A* and *B*-1 to *B*-11 on surface *B*. In addition, three surface *A* film, *S*-2, *S*-5, and *S*-9, each 0·25 in. long and centered approximately 0·75 in. from the center line, were used to check the departure of the surface temperature from the one dimensional requirement. Further details of the model and instrumentation can be found in [19].

Surface *B* was given a single coat of sprayed matt-black cellulose paint to improve the infra-red radiation absorption rate, and to serve as an absorption layer for the conversion of infra-red radiation to sensible heat. In this way, the films bounded a region of pure conduction without the complication of distributed heat source effects. The painted surface *B*, carrying the wiring, was fitted with a vented cover of 0·003 in. thick celluloid in order to make it aerodynamically cleaner, especially during oscillation, so that transition and the higher associated heat-transfer rate would be prevented.

The wind-tunnel used was a low speed, low turbulence, temperature controlled, blow-down installation (contraction ratio 81) converted to an open-ended working section type on account of the bulky nature of the mounting of the model and its oscillatory drive. The working section was a 4 in. i.d. polished plexiglass tube with a wall thickness of $\frac{3}{32}$ in.

The working section velocity was measured with a small pitot-static tube connected to a sloping tube manometer containing absolute ethyl alcohol, the meniscus of which was observed through a travelling microscope. The error in setting a velocity $U = 5$ ft/s was estimated to be of the order of 2 per cent. The lowest velocity used, $U = 2{\cdot}5$ ft/s, was obtained from the extrapolated calibration curve of a constant temperature platinum hot wire.

The model sting was clamped in the chuck of a modified, high quality jig saw, with an electrical strike contact switch to indicate phase relationships up to the maximum attainable

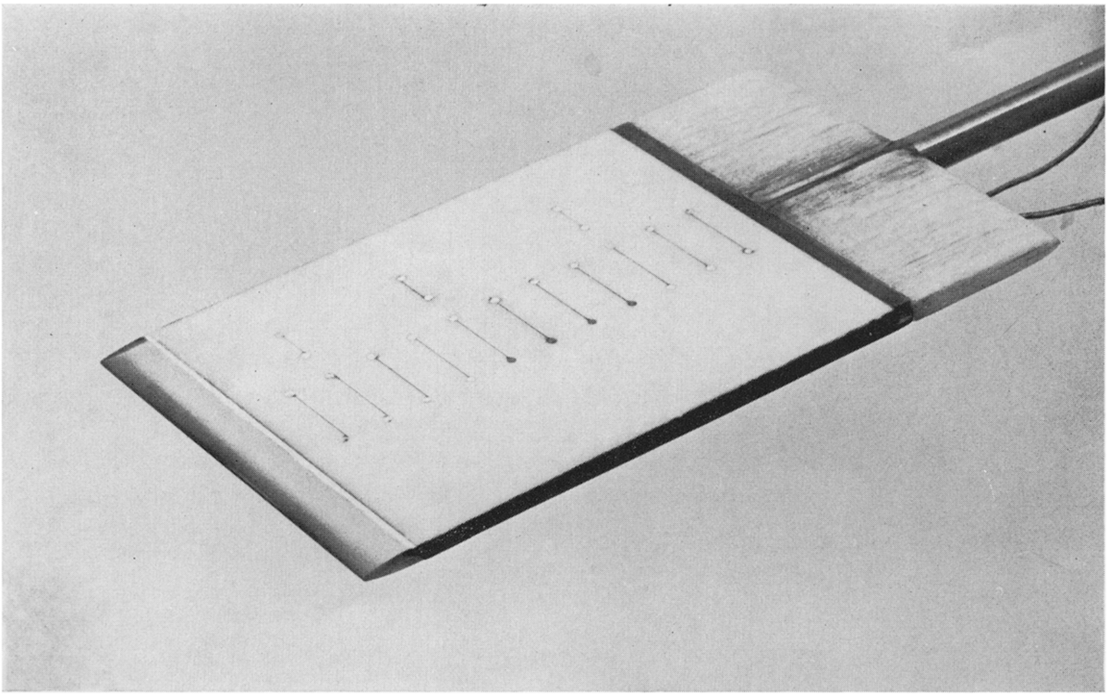

FIG. 1. Flat plate model, airstream surface *A*.

oscillation frequency of 60 Hz. Oscillatory motion was produced by a slider-crank arrangement, with a crank radius $r = 0{\cdot}493$ in. (equal to the linear motion amplitude) and a connecting rod length $l = 2{\cdot}050$ in., with the resultant plate velocity, including the steady stream velocity U_∞, being

$$U(t) = U_\infty \left\{1 + \frac{\omega r}{U_\infty} \sin \omega t \times \left[1 + \frac{\cos \omega t}{(17{\cdot}3 - \sin^2 \omega t)^{\frac{1}{2}}}\right]\right\}.$$

The deviation from true sinusoidal motion produced a maximum plate velocity $u_{p_{max}}$ which was 6 per cent greater than the ideal value ωr, and occurred at $\omega t = 77°$ instead of 90°.

The jig-saw was solidly bolted to the final contraction section of the tunnel, with the black surface B of the model uppermost. Four 250 W infra-red heating lamps were adjusted to give a radiant energy flux as uniform as possible over the area occupied by the model at any instant. Readings from a vacuum thermocouple showed that the relative radiation field strength was within ±5 per cent of the mean value.

Steady temperature data from Wheatstone bridges containing the film thermometers was obtained from a pair of Rubicon potentiometers, each fitted with an external mirror galvanometer with a sensitivity of 0·1°F per scale division. Unsteady temperature signals during oscillation from surface A were amplified by a calibrated Tektronix Type 122 low level pre-amplifier. Use of the push–pull input proved very satisfactory in rejecting noise associated with the oscillatory drive and heating lamps. With a dummy, unpowered bridge circuit (containing the B surface film opposite the one from which unsteady measurements were being taken) connected to to the second input, the resulting noise referred to the input at a gain of 1000 and an upper frequency cut-off of 250 Hz, was approximately one microvolt peak to peak, and remained essentially random in nature during model oscillation.

The pre-amplifier output was connected to the upper beam of a Tektronix Type 522 dual beam oscilloscope, the lower beam being connected to display the surface B temperature and the timing mark indicating the phase relation between temperature and velocity. Data from the oscilloscope were recorded on 70 mm Tri-X film, with the camera flash contacts used to trigger the traces. The film records were projected at a magnification of 10 diameters and subjected to a 12 point Fourier analysis.

4. PROCEDURE

Unsteady data reduction required the value of the thermal diffusivity, χ, of the plate material. This was determined in the laboratory using a closely similar plate equipped on both surfaces with copper–constantan thermocouples (made from 0·001 in. dia. wire) and attached with the minimum necessary amount of solder to platinum film spots fired on the surface. After spraying one surface matt-black, the model was installed in a vacuum chamber and suddenly exposed on the black side to uniform radiation from infra-red-lamps directed through glass windows. After the initial transient had decayed, the constant temperature difference between the two surfaces produced a value of $\chi = 6{\cdot}23 \times 10^{-6}$ ft²/s using a standard heat conduction result [20].

An oscilloscope display of the hot wire output

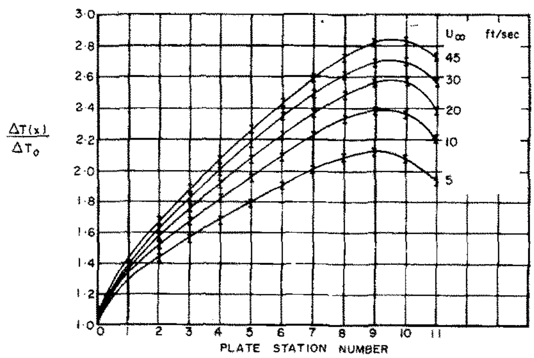

FIG. 2. Surface temperature distribution for $\Delta T_{11} = 30, 40, 60$ and 80°F.

showed that the boundary layer over the rear 1 in. portion of the ceramic section was laminar when the plate was oscillating up to the highest frequency of 60 Hz, with $U_\infty = 2{\cdot}5$–45 ft/s (the highest value used in the experiment).

The platinum films were calibrated a pair at a time in an air bath using a pair of Wheatstone bridges connected singly and in opposition as described in [19]. In the wind tunnel, the same circuitry was used for measuring the model surface temperature $\Delta T(x)$ and the temperature difference $\Delta_1 t(x)$ across its thickness by electrical subtraction, with the results shown in Figs. 2 and 3, for $\Delta T_{11} = 80°\text{F}$ at the trailing edge.

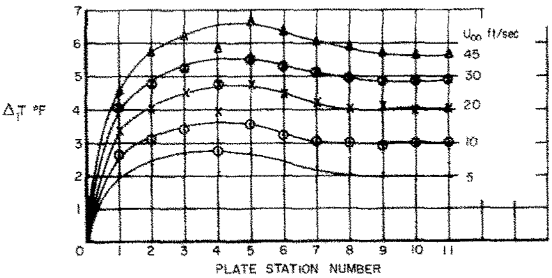

FIG. 3. Temperature difference measurements, $\Delta_1 T$, for $\Delta T_{11} = 80°\text{F}$.

The Schwarz–Christoffel transformation (see Appendix) was used to determine steady state normal temperature-gradient $(\partial T/\partial n)_s$ at surface A, and the results, for $\Delta T_{11} = 80°\text{F}$ (the principal value used during the unsteady experiments), have been correlated as shown on Fig. 4 by means of the non-dimensional parameter

$$\left(\frac{\partial T}{\partial n}\right)_s \sqrt{\left(\frac{\nu x}{U_\infty}\right)} \Big/ \Delta T.$$

This parameter is simply $Nu/Re^{\frac{1}{2}}$ multiplied by the ratio of the thermal conductivity of air to that of the ceramic. In order to correlate $(\partial T/\partial n)_s$ for all value of ΔT_{11}, the parameter

$$(1 + \lambda \Delta T)\left(\frac{\partial T}{\partial n}\right)_s \sqrt{\left(\frac{\nu x}{U_\infty}\right)} \Big/ \Delta T$$

with $\lambda = 0{\cdot}0065$ produced a better fit (Fig. 4). It is possible that λ represents the coefficient of

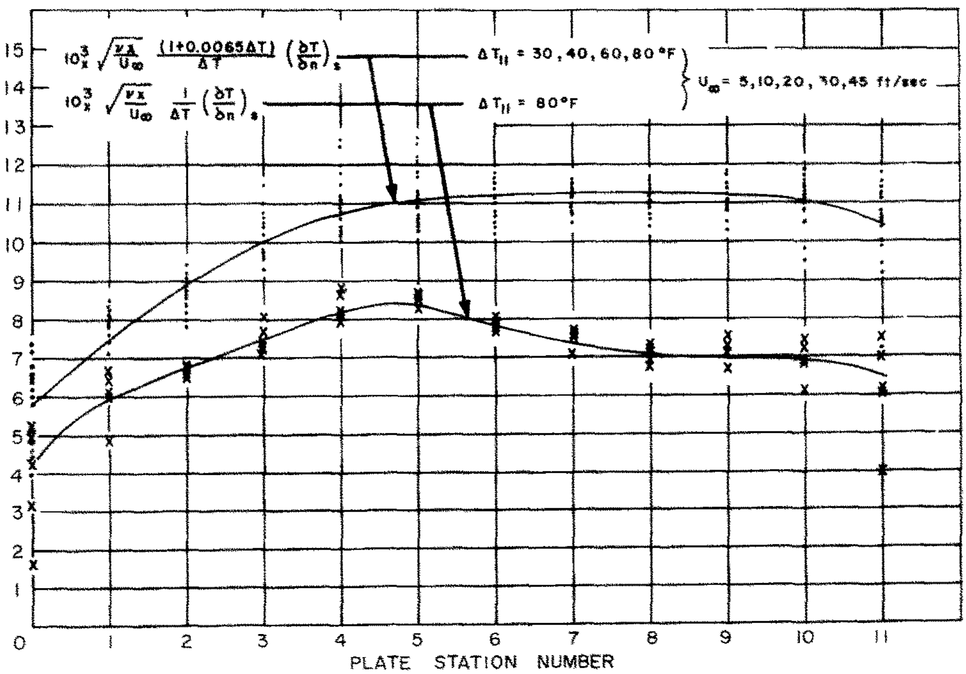

FIG. 4. Correlation of steady state heat transfer results.

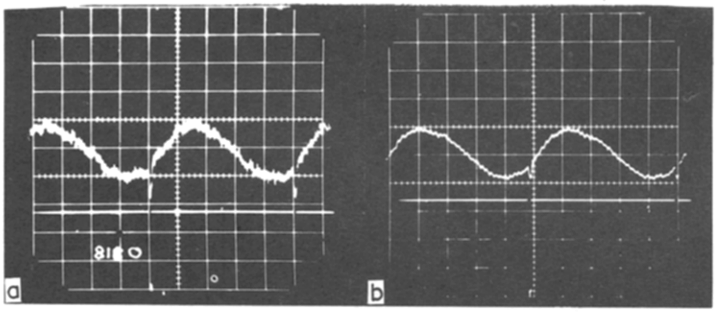

$f = 0{\cdot}94$ Hz, $\delta_1 T = 0{\cdot}0037$°F
$U_\infty = 45$ ft/s, $\epsilon = 0{\cdot}00553$
$S = 0{\cdot}00820$, $H = 0{\cdot}00516$

$f = 1{\cdot}95$ Hz, $\delta_1 T = 0{\cdot}0086$°F
$U_\infty = 10$ ft/s, $\epsilon = 0{\cdot}0518$
$S = 0{\cdot}0767$, $H = 0{\cdot}0289$

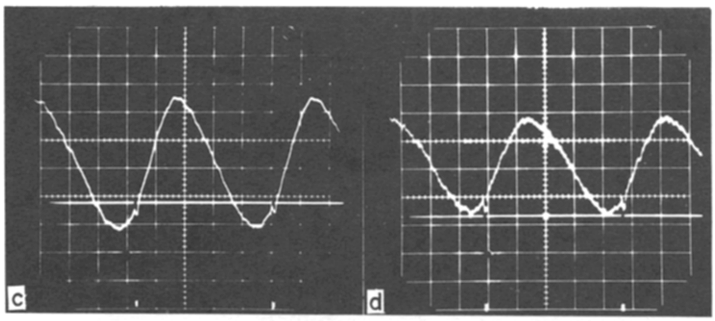

$f = 4{\cdot}18$ Hz, $\delta_1 T = 0{\cdot}020$°F
$U_\infty = 5$ ft/s, $\epsilon = 0{\cdot}221$
$S = 0{\cdot}328$, $H = 0{\cdot}130$

$f = 10{\cdot}5$ Hz, $\delta_1 T = 0{\cdot}015$°F
$U_\infty = 20$ ft/s, $\epsilon = 0{\cdot}139$
$S = 0{\cdot}205$, $H = 0{\cdot}0910$

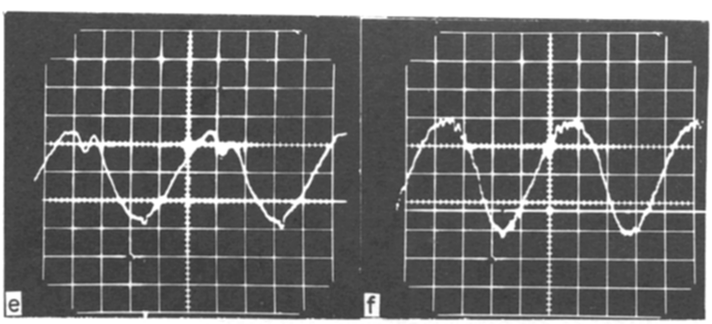

$f = 20{\cdot}8$ Hz, $\delta_1 T = 0{\cdot}027$°F
$U_\infty = 10$ ft/s, $\epsilon = 0{\cdot}550$
$S = 1{\cdot}36$, $H = 0{\cdot}278$

$f = 45{\cdot}7$ Hz, $\delta_1 T = 0{\cdot}036$°F
$U_\infty = 5$ ft/s, $\epsilon = 2{\cdot}42$
$S = 3{\cdot}59$, $H = 0{\cdot}875$

FIG. 5. Examples of unsteady temperature traces for $\Delta T_{11} = 80$°F.

thermal conductivity change with temperature for the ceramic, i.e. $= K_0(1 + \lambda \Delta T)$ where K_0 is the conductivity at $\Delta T = 0$. Support for a positive value of λ for insulating heterogeneous materials, such as Parian, is given in [21]. For the Schwarz–Christoffel integration, the change in K at a particular film station with respect to the adjacent stations would be approximately ± 3 per cent an $\Delta T_{11} = 80°F$ with $(d/dx)\,\Delta T \simeq 20°F/in.$). Its effect, if present, was therefore neglected, considering the probable error (0·2°F) in $\Delta_1 T$.

Unsteady temperature measurements at surface A along the plate length were taken at plate oscillation frequencies of 1–60 Hz through the same ranges of U_∞ and ΔT_{11} as used in the steady experiments. Examples of the oscilloscope traces obtained are shown in Fig. 5. Small breaks in the steady surface B trace correspond to the plate being in its most forward position and at the maximum value of $U(t)$. With appropriate incorporation of calibration factors for the film thermometer, preamplifier gain and oscilloscope setting, data from the projected film record was Fourier analyzed in a digital computer program to provide temperature amplitude information for the unsteady temperature expression :

$$\delta_1 T = \sum_{m=1}^{5} (\delta_1 T)_m \sin m\omega t + \sum_{n=1}^{6} (\delta_1 T)_n \cos n\omega t.$$

Under the conditions of the present experiment, and with the experimentally determined x-dependence of $\delta_1 T$, it is shown in [19] that the unsteady normal temperature gradient at surface A is given by

$$\frac{\partial T}{\partial n} = \sqrt{\left(\frac{\omega}{\chi}\right)}\left[\sum_{m=1}^{6} (\sqrt{m})(\delta_1 T)_m \sin\left(m\omega t + \frac{\pi}{4}\right) + \sum_{n=1}^{6} (\sqrt{n})(\delta_1 T)_n \cos\left(n\omega t + \frac{\pi}{4}\right)\right].$$

The maximum value of the temperature gradient $(\partial T/\partial n)_u$ and its phase ϕ_Q with respect to the plate velocity were determined by Newton's method.

The experimental results for comparison with theoretical predictions are shown in Figs. 6–8. A few unsteady temperature traces exhibited a highly localized departure from the generally smooth curve. This deviation was locally smoothed since it sometimes occurred between the measuring ordinates so that it could not be taken into account with a 12 point Fourier analysis. An idealized analysis showed that such neglect of a typical deviation resulted in an error in $(\partial T/\partial n)_u$ of less than 3 per cent.

The reduced data to this point showed a changing trend for $1{\cdot}5 < S < 6$, and it was considered desirable to confirm these results, and also to obtain data for $S > 6$. Therefore, since the surface B film thermometer leads were broken, the trailing edge temperature was measured at film A-10 and denoted by ΔT_{10}. For these extended results, a value of $U_\infty = 2{\cdot}5$ ft/s was set using the calibrated hot wire anemometer, and for $\Delta T_{10} = 85°F$, unsteady data was obtained up to $S = 20$ from the remaining serviceable A-films. The corresponding steady state temperature gradient values were obtained by

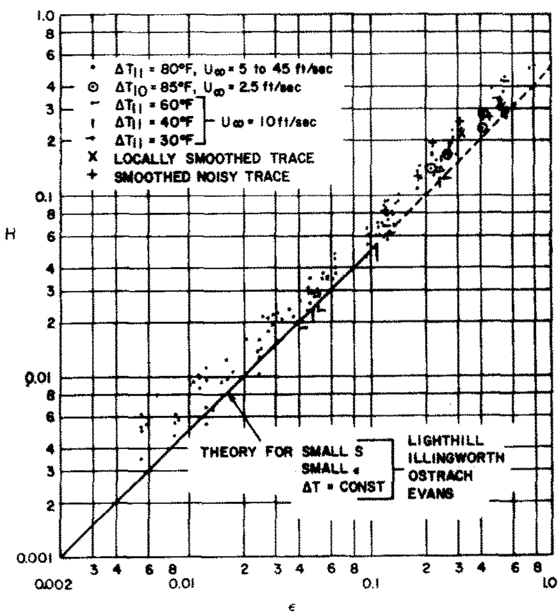

FIG. 6. Experimental results for $S < 1{\cdot}5$ compared with theory.

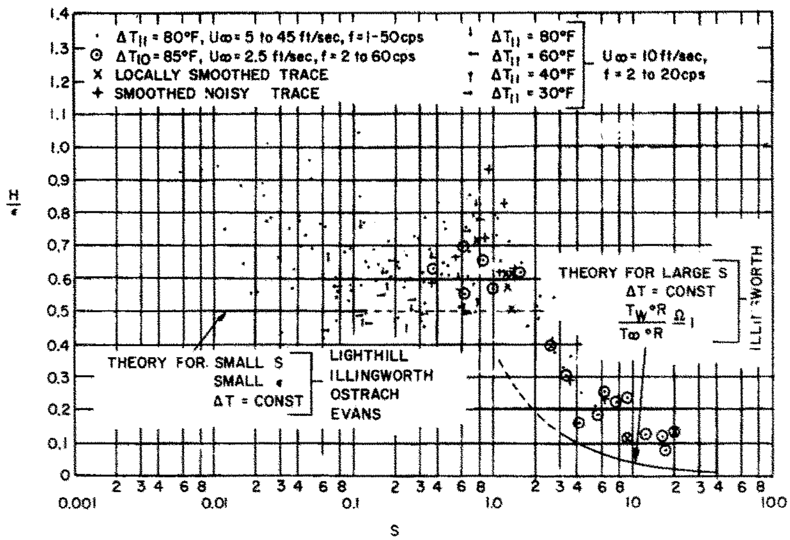

FIG. 7. Comparison of all experimental heat transfer results with theory.

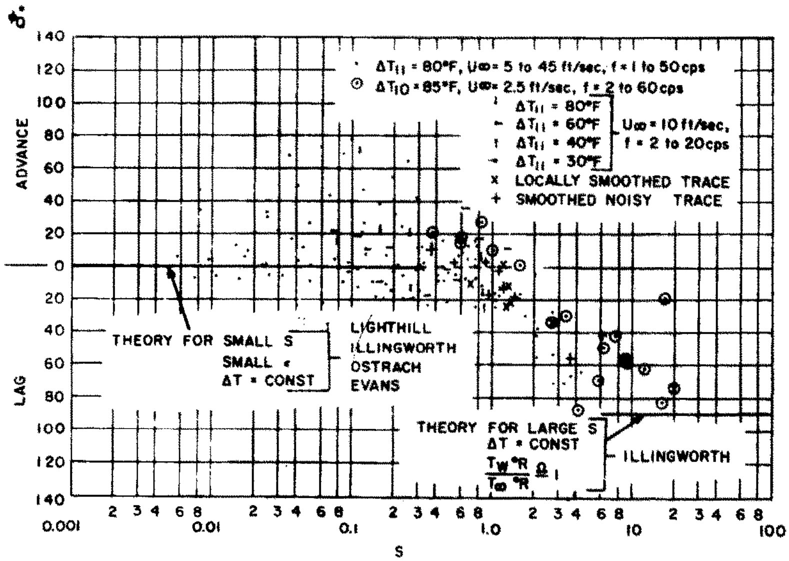

FIG. 8. Variation with S of phase of heat transfer, ϕ_Q, with respect to velocity.

extrapolation of the reasonably well correlated results plotted in Fig. 4.

For detecting changes in the time-averaged heat transfer during oscillation, a double difference method was used, as follows. A steady state experiment was repeated and the bridge potentiometer was adjusted to null the bridges' output corresponding to $\Delta_1 T$. The plate was then oscillated, and the change in potentiometer output required to produce the new null was recorded. In this way, with a galvanometer sensitivity of 0·1°F per division, it was estimated that changes of 0·05°F in $\Delta_1 T$ could be reliably detected. Several measurements up to $S \doteq 2$ ($f = 10$ Hz) did not show any measurable change in $\Delta_1 T$ after more than 1 min of plate oscillation, indicating no change in the steady state heat transfer. It was also consistently observed that the mean surface temperature did not change during oscillation. The above-mentioned surface B film lead breakage prevented measurements for $S > 2$.

5. DISCUSSION OF THE RESULTS

The curves of the surface temperature distribution, $\Delta T(x)$, (Fig. 2), show a weak Reynolds number dependence through the velocity, but are independent of the temperature level of operation ΔT_{11}, as would be expected from the linear nature of the energy equation. The decrease in $\Delta T(x)$ in the region of stations 10 and 11 is attributed to conduction in the rear metal supporting bar and sting to which the ceramic test length was attached.

Steady state measurements indicated that $\Delta_1 T(x)$ (Fig. 3) was essentially constant, for each value of ΔT_{11}, over the rear portion of the model. This (perhaps fortuitous) fact simplified the data reduction to obtain the steady state normal temperature gradient at surface A, since it allowed the convenient use of a constant boundary condition at infinity in the plane resulting from application of the Schwarz–Christoffel transformation.

Theoretical predictions for steady flow for the cases $\Delta T(x) =$ constant and $\Delta T \propto x^{\frac{1}{2}}$ show that $Nu/Re^{\frac{1}{2}} =$ constant. Although, with non-constant $\Delta T(x)$, the results of all tests correlated reasonably well on the basis of an equivalent parameter (modified by a small parameter λ possibly representing the coefficient of thermal conductivity change with temperature of the ceramic), only those results between stations 5 and 10 (Fig. 4) appeared approximately constant, with the results upstream of station 5 being clearly dependent on the Reynolds number through the distance x from the leading edge. A value of $\lambda = 0{\cdot}0065$ appeared to give the best constant correlation over stations 5–10. It should be borne in mind that the maximum unsteady normal surface temperature gradient, $(\partial T/\partial n)_u$ was to be compared with $(\partial T/\partial n)_s$ at the same station and ΔT, so that effects due to certain factors, such as the possible dependence of the ceramic thermal conductivity on temperature, would tend to cancel. Although the energy input from the heating lamps was constant to within ± 5 per cent of a mean, the steady state heat transfer, as indicated by $(\partial T/\partial n)_s$, was not constant along the test length due to conduction within the model and along its support sting.

For $S < 1{\cdot}5$ the parameter H was found to be a linear function of ϵ (Fig. 6), while the results for the full experimental range (Fig. 7) show that $H/\epsilon \propto 1/S$ approximately for $S > 1{\cdot}5$. Both results are, respectively, in good qualitative agreement with theory for small S and large S. The experimental results suggest that both parts of the theory can be satisfactorily joined at $S = 1{\cdot}5$, a fact that was not determinable by Illingworth in his analysis [22] of the heat-transfer case, although he was able to estimate a joining value of $S = 0{\cdot}59$ for the skin friction solutions.

It is also of interest to note that values of $H = 0{\cdot}75$ approximately were measured in the neighborhood of $\epsilon = 1$ and $S = 1$. The scatter of the results, shown more realistically on Fig. 7, is partially attributed to the fact that unsteady heat-transfer information had to be extracted by differentiation of temperature data.

The quantitative deviation between experiment and theory for H/ε vs. S was approximately 35 per cent. Estimates were made for the effect caused by errors in the measurement of the various temperatures and the value obtained for the ceramic thermal diffusivity, film thermometer misplacement, departure from the one dimensional temperature requirement, and the non-sinusoidal plate motion. Summation of the magnitudes of these error estimates amounted to less than 20 per cent, and was, in any case, highly pessimistic, since most of the errors were random. However, the fact that experimental limitations produced $\Delta T \propto x^{\frac{1}{2}}$ approximately, while the theoretical treatments were restricted to constant ΔT, was probably the major contributing cause to the extent of the deviation. However, the x-dependence of ΔT did not upset the correlation based on H/ϵ, presumably because the boundary layer has the ability to adjust to a new temperature environment in a relatively short distance, of the order of a few boundary-layer thicknesses.

The results for the phase relation between heat-transfer rate and velocity (Fig. 8) show considerable scatter on account of data differentiation and the relatively coarse (30°) grid used in the 12-point Fourier analysis. However, for $S < 1{\cdot}5$, over 70 per cent of the points fell within $\pm 20°$ of the theoretical in-phase prediction. For $S > 1{\cdot}5$, the heat transfer phase lag increased with S, and approached the theoretical value of 90° at $S = 20$.

Finally, theoretical predictions were experimentally confirmed in that no change in the time-averaged heat transfer during plate oscillation was detectable, to within 3 per cent, for $S \leqslant 2$.

6. CONCLUSIONS

1. Theoretical predictions for laminar heat transfer from a flat plate oscillating in air over a wide range of Strouhal number have been qualitatively confirmed by experiment. In particular, H/ϵ was found to be essentially independent of S for $S < 1{\cdot}5$, whereas $H/\epsilon \propto 1/S$ for $S > 1{\cdot}5$, with no change in time-averaged heat transfer during oscillation being detectable for $S \leqslant 2$. In addition, values of $H = 0{\cdot}75$ were measured in the neighborhood of $\epsilon = 1$ and $S = 1$.

2. For $S < 1{\cdot}5$, the heat-transfer rate was essentially in phase with the velocity as required by theory, and, for $S > 1{\cdot}5$, the lag in heat-transfer rate progressively increased, approaching the theoretical value of 90° at $S = 20$.

3. The experimental results indicated that the heat transfer theories for both small and large S could be satisfactorily joined at $S = 1{\cdot}5$, a fact itself not determinable from the theories.

4. The quantitative deviation between experiment and theory was attributed principally to the fact that practical limitations prevented the use of a constant plate surface temperature, as required by theory. However, this condition did not upset the experimental correlation based on H/ϵ.

REFERENCES

1. R. J. NICKERSON, The effect of free stream oscillations on the laminar boundary layer on a flat plate, M.I.T., Sc.D. Thesis (May 1957).
2. P. G. HILL and A. H. STENNING, Laminar boundary layers in oscillatory flow, *Trans. Am. Soc. Mech. Engrs* **82D** (3), (Sept. 1960).
3. M. V. MORKOVIN, New insights on transition in oscillating boundary layers. Keynote Address, Fluid Dynamics Symposium, McMaster University (1970); also AFOSR Scientific Report 70-1586 TR.
4. H. A. HAVEMANN and N. N. RAO, Heat transfer in pulsating flow, *Nature* **174**, 41 (July 1954).
5. R. S. WICK, Unsteady boundary layer and heat transfer phenomena– a literature survey, Cal. Inst. Tech. Rept. No. 20-279 (1955).
6. F. E. ROMIE, Heat transfer to fluids flowing with velocity pulsations, Ph.D. Thesis, Univ. Calif. (1956).
7. D. T. HARRJE, Effects of oscillating flow on heat transfer in a tube, Jet Prop. Lab. Cal. Tech. No. 20-362.
8. Heat transfer in oscillating flow, Princeton Univ. Aero. Eng. Dept. Rept. No. 483 (Oct. 1959).
9. Heat transfer in oscillating flow, Princeton Univ. Aero. Eng. Dept. Rept. No. 483b (Sept. 1960).
10. Heat transfer in oscillating flow, Princeton Univ. Aero. Eng. Dept. Rept. No. 483c (Sept. 1961).
11. R. LEMLICH, Effects of vibration on natural convective heat transfer, *Ind. Engng Chem.* **47**, 1175 (1955).
12. R. ANANTANARAYANAN and A. RAMACHANDRAN, Effect of vibration on heat transfer from a wire to air in parallel flow, *Trans. Am. Soc. Mech. Engrs* **80** (7), 1426–1432 (1958).

13. R. LEMLICH and C. K. HWU, Vibrations on forced convective heat transfer, *A.I.Ch.E.* 7, 102–105 (1961).
14. I. RABEN, The use of acoustic vibrations to improve heat transfer, Heat Transfer and Fluid Mechanics Inst., Univ. Southern Calif. (June 1961).
15. C. D. FEILER and E. B. YEAGER, Effect of large amplitude oscillations on heat transfer, NASA TR R-142 (1962).
16. R. LEMLICH, Vibration and pulsation boost heat transfer, *Chem. Engr.* **68** (10), 171–177 (1961).
17. N. A. EVANS, Heat transfer through the unsteady laminar boundary layer on a semi-infinite flat plate. Part I: Theoretical considerations. *Int. J. Heat Mass Transfer* **16**, 55–565 (1973).
18. G. N. SARMA, Unified theory for the solutions of the unsteady thermal boundary layer equations. *Proc. Camb. Phil. Soc.* **61**, 809–825 (1965).
19. N. A. EVANS, Sensitive platinum films for heat transfer measurement. Annual Inst. Soc. America Conference and Exhibit, New York (Oct. 1972).
20. H. S. CARSLAW and J. C. JAEGER, *Conduction of Heat in Solids*, p. 401. Clarendon Press, Oxford (1950).
21. W. D. KINGERY, *Introduction to Ceramics*, pp. 506–508. John Wiley, New York (1960).
22. C. R. ILLINGWORTH, The effects of a sound wave on the compressible boundary layer on a flat plate, *J. Fluid Mech.* **3**, Part 5 (1958).
23. P. M. MORSE and H. FESHBACH, *Methods of Theoretical Physics*, Part I, p. 371. McGraw-Hill, New York (1953).

APPENDIX

Mathematical Details of the Steady State Data Reduction

The model is placed in the $z = x + iy$ plane as shown in Fig. 9, and scaled for convenience, so that station 1 is at a distance unity from the origin. The appropriate Schwarz–Christoffel transformation to the $w = u + iv$ plane is given by

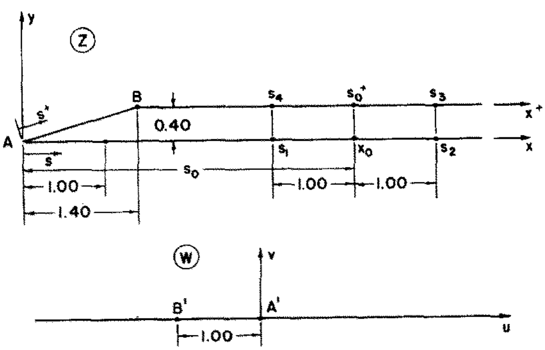

FIG. 9. Schwarz–Christoffel transformation for determining $(\partial T/\partial n)_s$.

$$\frac{\mathrm{d}w}{\mathrm{d}z} = Cw^{0.915}(1 + w)^{0.085}$$

and the plate lies along the real axis in the w-plane, where A and B transform to A' and B', respectively (Fig. 9), with the interior of the model mapping into the upper half of the plane. With B' at $w = -1$, the transformation scaling factor was determined by quadrature to be $C = 8.177$. For $|w| > 1$ (i.e. not too close to the plate leading edge A),

$$\frac{\mathrm{d}w}{\mathrm{d}z} \simeq 8.177w$$

giving $\ln w = 8.177z + K$, where K is an integration constant. Therefore on the plate boundary with $|z| = s$ as the contour distance from A, $u \propto e^{8.177s}$ for $s > 1.4$ to a good approximation.

The temperature gradient is given by

$$\frac{\partial T}{\partial y} = \left(\frac{\partial T}{\partial u}\right)_v \frac{\partial u}{\partial y} + \left(\frac{\partial T}{\partial v}\right)_u \frac{\partial v}{\partial y}.$$

Since

$$\frac{\mathrm{d}w}{\mathrm{d}z} = \frac{\mathrm{d}u + i\mathrm{d}v}{\mathrm{d}x + i\mathrm{d}y}$$

is purely real on the plate boundary, then $\partial u/\partial y = 0$ and $\partial v/\partial y = \mathrm{d}w/\mathrm{d}z$, so that the required gradient at the surface is

$$\left(\frac{\partial T}{\partial y}\right)_{y=0} = \left[\frac{\mathrm{d}w}{\mathrm{d}z}\left(\frac{\partial T}{\partial v}\right)_u\right]_{v=0}. \quad \text{(A.1)}$$

The solution for a potential function, T, is given [23] by

$$T(u, v) = \frac{v}{\pi} \int_{-\infty}^{+\infty} \left[\frac{T(u', 0)}{(u' - u)^2 + v^2}\right] \mathrm{d}u'$$

and it can be shown that

$$\left(\frac{\partial T}{\partial v}\right)_{v=0}(s) = \frac{1}{\pi} \int_{-\infty}^{+\infty} \left(\frac{\partial T}{\partial s'}\right) \frac{\mathrm{d}s'}{[u(s') - u(s)]}$$

where the principal value of the integral is required, and the integration is now performed in the physical z-plane.

For a particular station $x = x_0$ where $s = s_0$ (Fig. 9), and considering the behavior of the approximation $u(s) \propto e^{8.177s}$ ($s > 1.4$), it is sufficient to consider the variation of $u(s') - u(s_0)$ only in the range $(s_0 - 1) < s < (s_0 + 1)$ on the x-axis, and $(s_0^+ - 1) < s^+ < (s_0^+ + 1)$ on the x^+-axis.

$$\therefore \left(\frac{\partial T}{\partial v}\right)_{v=0}(s_0) = \int_{-\infty}^{+\infty} \left(\frac{\partial T}{\partial s'}\right) \frac{\mathrm{d}s'}{[u(s') - u(s_0)]}$$

$$= \frac{1}{\pi} \frac{[T(s_1) - T(s_4)]}{-u(s_0)} + D + E \quad \text{(A.2)}$$

where

$$D = \frac{1}{\pi}\int_{s_3}^{s_4}\left(\frac{\partial T}{\partial s'}\right)^+ \frac{ds'}{[u(s') - u(s_0)]}$$

and

$$E = \frac{1}{\pi}\int_{s_1}^{s_2}\left(\frac{\partial T}{\partial s'}\right)\frac{ds'}{[u(s') - u(s_0)]}$$

with

$$s_3 < s_4 < 0 < s_1 < s_2.$$

For $s \geqslant 0$,

$$s = \frac{1}{8{\cdot}177}\left[\int_0^1 \frac{dw}{w^{0{\cdot}915}(1+w)^{0{\cdot}085}} + \int_1^u \frac{dw}{w}\left(1 - \frac{0{\cdot}085}{w} + \ldots\right)\right]$$

$$= \frac{1}{8{\cdot}177}\left[K_1 + \ln u + 0{\cdot}085\, O\left(\frac{1}{u}\right)\right]$$

where K_1 is a constant determined by quadrature from the first and second integrals, and there follows $u(s) = e^{8.177s - K_1}$. Similarly, for $s \leqslant 0$ on the slightly longer path $s = s^+$, then $u(s^+) = e^{-8{\cdot}177s^+ + K_2}$. With these evaluations for $u(s)$ and $u(s^+)$, the integrals D and E were computed using polynomial representationr for $\partial T/\partial s$ and $(\partial T/\partial s)^+$, with the final solution being given by equations (A.1) and (A.2).

TRANSFERT THERMIQUE A TRAVERS LA COUCHE LIMITE LAMINAIRE INSTATIONNAIRE SUR UNE PLAQUE PLANE SEMI-INFINIE—II. RESULTATS EXPERIMENTAUX SUR UNE PLAQUE OSCILLANTE

Résumé—Une plaque plane de céramique chauffée par l'extérieur sur les faces de laquelle sont fixés des thermomètres à résistance film de platine à court temps de reponse, est utilisée pour comparer l'amplitude du flux thermique additionnel non permanent δq_w pendant l'oscillation dans son propre plan dans un courant d'air parallèle permanent, de vitesse U_∞, avec le flux thermique correspondant à l'état permanent, q_{ws}, sans oscillation.

La fréquence d'oscillation de la plaque f varie entre 1 et 60 Hz; le domaine correspondant du nombre de Strouhal $S = \omega x/U_\infty$ (x est la distance au bord d'attaque, $\omega = 2\pi f$) allant de 0,996 à 20 et celui du rapport de vitesse $\varepsilon = U_{p_{max}}/U_\infty$ ($U_{p_{max}}$ est la vitesse maximale de la plaque) s'étendant de 0,005 à 6,5.

L'amplification des signaux électriques périodiques correspondant aux amplitudes de température dans le domaine de 0,0017 et 0,022°C montre que les tendances qualitatives de plusieurs théories sur le comportement et le déphasage (par rapport à $U_{p_{max}}$) de H/ε (où $H = \delta q_w/q_{ws}$) pour à la fois S petit et grand, sont confirmées par l'expérience. H/ε est essentiellement constant et en phase pour $S < 1{,}5$ tandis que pour $S > 1{,}5$, $H/\varepsilon \propto 1/S$ avec un déphasage qui s'approche progressivement de 90°. De plus, pour un nombre limité d'essais on ne détecte aucun changement dans le transfert thermique permanent jusqu'à la valeur $S = 2$.

WÄRMEÜBERTRAGUNG DURCH DIE INSTATIONÄRE LAMINARE GRENZSCHICHT AN EINER HALBUNENDLICHEN FLACHEN PLATTE—TEIL II. EXPERIMENTELLE ERGEBNISSE MIT EINER OSZILLIERENDEN PLATTE

Zusammenfassung—Eine von aussen beheizte flache Keramikplatte, die auf beiden Seiten mit schnell ansprechenden Platin-Film-Widerstandsthermometern versehen war, wurde verwendet um die Amplitude des zusätzlichen instationären Wärmestroms δq_w während der Oszillation in ihrer eigenen Ebene in einem stationären parallelen Luftstrom von der Geschwindigkeit U_∞ zu vergleichen mit dem korrespondierenden stationären Wärmestrom q_{ws} ohne Oszillation.

Die Frequenz f der Plattenschwingung lag im Bereich 1 bis 60 Hz, die korrespondierende Grösse der Strouhal-Zahl $S = \omega_x/U_\infty$ ($\omega = 2\pi f$, x ist der Abstand von der Anströmkante) zwischen 0,006 und 20 und das Geschwindigkeitsverhältnis $\varepsilon = U_{p\max}/U_\infty$ ($U_{p\max}$ ist die maximale Geschwindigkeit der Platte) lag zwischen 0,005 und 6,5.

Die Verstärkung der periodischen elektrischen Signale, die Temperaturamplituden entsprechen von 0.003 bis 0,022°C, zeigen, dass qualitativ die Tendenz mehrerer existierender Theorien für das Verhalten und die Phasenverschiebung (unter Beachtung von $u_{p\max}$) von H/ε (wobei $H = \delta q_w/q_{ws}$) sowohl für grosse als auch kleine S durch das Experiment bestätigt wird. H/ε war im wesentlichen konstant und in Phase für $S < 1{,}5$, wobei gilt: $S > 1{,}5$, $H/\varepsilon \cong 1/s$ mit einer Phasenverzögerung, die sich 90° nähert. Für eine begrenzte Anzahl von Versuchen war keine Änderung des stationären Wärmeübergangs im Bereich $S > 2$ feststellbar.

ПЕРЕНОС ТЕПЛА ЧЕРЕЗ НЕСТАЦИОНАРНЫЙ ЛАМИНАРНЫЙ ПОГРАНИЧНЫЙ СЛОЙ. НА ПОЛУБЕСКОНЕЧНОЙ ПЛОСКОЙ ПЛАСТИНЕ. 2. РЕЗУЛЬТАТЫ ОПЫТОВ С КОЛЕБЛЮЩЕЙСЯ ПЛАСТИНОЙ.

Аннотация—Нагреваемая снаружи плоская керамическая пластина, на обеих сторонах которой установлены чувствительные пленочные термометры сопротивления из платины, использовалась для сравнения амплитуды дополнительной скорости нестационарного переноса δq_w при колебаниях в собственной плоскости в стационарном параллельном потоке воздуха, движущимся со скоростью U_∞, с соответствующей стационарной скоростью переноса тепла q_{ws} при отсутствии колебаний.

Частота колебаний пластины f изменялась от 1 до 60 гц, соответствующий диапазон уисла Струхаля $S = \omega x/U_\infty$ (где $\omega = 2\pi f$, x-расстояние от передней кромки) составлял 0,006–20, а диапазон безразмерной скорости $\epsilon = u_{p\max}/U_\infty$ (где $u_{p\max}$ максимальная скорость пластины) был 0,005–6,5.